The Journal of Neuroscience, March 1, 2001, *21*(5):1481–1489

Insulin-Like Growth Factor-I Overexpression Attenuates Cerebellar Apoptosis by Altering the Expression of Bcl Family Proteins in a Developmentally Specific Manner

Dionisios Chrysis, Ali Suha Calikoglu, Ping Ye, and A. Joseph D'Ercole

Department of Pediatrics, The University of North Carolina, Chapel Hill, North Carolina 27599-7220

In studies of transgenic (Tg) mice that overexpress insulin-like growth factor-I (IGF-I) exclusively in the CNS, we demonstrated a dramatic increase in cerebellar granule cell number that appeared to be attributable predominantly to enhanced survival. IGF-I anti-apoptotic actions are well established in cultured neurons, but comparable studies *in vivo* are few. Using the same Tg mice, therefore, we set out to document IGF-I anti-apoptotic effects during cerebellar development and to probe IGF-I signaling mechanisms. Compared with cerebella (CBs) of non-Tg littermates, those of Tg mice had fewer apoptotic cells at postnatal day 7 (P7) and showed a similar tendency at P14 and P21. At each age studied, procaspase-3 and caspase-3 were decreased in CBs of Tg mice. The caspase-3 decline was accompanied by decreases in the 85 kDa fragment of Poly(ADP-ribose) polymerase, a known product of caspase cleavage, suggesting decreased caspase activity. At P7 decreased apoptosis in Tg mice was associated with increased expression of the anti-apoptotic Bcl genes, Bcl-x_L and Bcl-2. The mRNA expression of the proapoptotic Bcl genes, Bax and Bad, also was increased, but no changes were observed in the abundance of their proteins. At P14 Bcl-xL and Bcl-2 expression were similar in normal and Tg mice; Bax mRNA was unchanged in Tg mice, but its protein abundance was decreased, and both Bad mRNA and protein abundance were decreased. At P21 Bcl-xL and Bcl-2 expression were unchanged, but Bax and Bad expression were decreased. Our data show that IGF-I exerts anti-apoptotic actions during cerebellar development, and thereby alters the magnitude of naturally occurring apoptosis. IGF-I appears to affect multiple steps in the apoptotic pathway in a developmentally specific manner. IGF-I decreases caspase-3 availability and activity, increases the expression of anti-apoptotic Bcl-x_L and Bcl-2 during early postnatal development, and decreases proapoptotic Bax and Bad expression at later developmental stages.

Key words: IGF-I; apoptosis; cerebellum; development; transgenic mice; Bcl; Bcl-2; Bcl-x_L; Bad; Bax; caspase-3; Poly(ADP-ribose) polymerase

Insulin-like growth factor-I (IGF-I) plays a significant role in the stimulation of brain development (D'Ercole et al., 1996). IGF-I overexpression in the brains of transgenic (Tg) mice results in brain overgrowth (Carson et al., 1993; Ye et al., 1995, 1996) that is characterized by an increase in neuron and oligodendrocyte number and a marked increase in myelination. The increase in cell number in IGF-I Tg mice appears to be attributable to both stimulation of proliferation and an inhibition of apoptosis. Mice with targeted disruptions of both IGF-I alleles have small brains with decreased myelination and a reduction or absence in certain neuron populations (Baker et al., 1993; Liu et al., 1993), and mice that lack expression of the type I IGF receptor have a similar phenotype (Baker et al., 1993; Liu et al., 1993). Many studies of cultured cells (Matthews and Feldman, 1996; Baserga et al., 1997), including those of cultured neurons and oligodendrocytes (Baker et al., 1999; Ye and D'Ercole, 1999), demonstrate that IGF-I is capable of promoting cell survival. Investigations into whether IGF-I acts *in vivo* to inhibit apoptosis, however, are few.

In studies of one of our lines of IGF-I Tg mice, we obtained evidence indicating that IGF-I stimulates cerebellar overgrowth primarily by inhibiting apoptosis (Ye et al., 1996). These mice carry a fusion gene that uses the mouse 5′ genomic regulatory region of the IGF-II gene to drive a human IGF-I cDNA (IGF-II/IGF-I Tg mice). This transgene is expressed throughout the brain beginning about the time of birth and exhibits highest expression in cerebellum (CB). Compared with normal littermates, the brains of heterozygous IGF-II/IGF-I Tg mice exhibit overgrowth from the second week of postnatal life with the CB exhibiting the greatest increase in size, such that by postnatal day 50 (P50) cerebellar weight is increased by 90%. The increased weight is attributable to an increase in the total number of granule and Purkinje cells (82 and 20% increases, respectively). Granule cell proliferation is modestly increased only at P15, making it unlikely that it is sufficient to account for the nearly twofold increase in granule cell number. Increased cell survival, therefore, appears to account for the increased cerebellar granule cell number. Several other studies of intact mice provide evidence consistent with IGF-I anti-apoptotic actions on neurons: (1) IGF-I gene expression is low in the Purkinje cell degeneration (pcd) mice, a mutant mouse line characterized by increased cerebellar apoptosis (Zhang et al., 1997), and (2) IGF-I treatment before experimental cerebral ischemia attenuates apoptosis in hippocampal neurons (Tagami et al., 1997).

Received Aug. 28, 2000; revised Nov. 28, 2000; accepted Dec. 5, 2000.

This work was supported by a Lawson–Wilkins Pharmacia & Upjohn Research Fellowship Award (D.C.) and by National Institutes of Health Grants HD08229 (A.J.D.) and DK-02506 (A.S.C.).

Correspondence should be addressed to Dr. A. Joseph D'Ercole, Department of Pediatrics, CB# 7220, University of North Carolina, Chapel Hill, NC 27599-7220. E-mail: joseph_d'ercole@unc.edu.

Dr. Chrysis' present address: Department of Woman and Child Health, Pediatric Endocrine Unit, Astrid Lindgren Children's Hospital, Q2: 08, Karolinska Institute, Stockholm, Sweden SE-171 76.

The mechanisms by which IGF-I prevents cultured cells from entering a death program have not been defined, and both the phosphatidylinositol 3′-kinase (PI3-K) and the mitogen-activated protein kinase (MAP-K) pathways (Kulik et al., 1997; Parrizas et al., 1997) have been implicated. Furthermore, a number of *in vitro* studies link IGF-I actions to the Bcl family of proteins, but these findings are somewhat discrepant. For example, IGF-I inhibition of apoptosis is associated with: (1) increased Bcl-x_L expression and action (Singleton et al., 1996; Parrizas and LeRoith, 1997); (2) increased Bcl-2 expression (Minshall et al., 1997); (3) suppressed interleukin-1β-converting enzyme (caspase)-mediated cell death, apparently through a mechanism independent of the expression of Bcl-2, Bcl-x_L, and Bax (Jung et al., 1996), and (4) an inactivation of Bad by phosphorylation (del Peso et al., 1997; Dudek et al., 1997). It seems likely that IGF-I anti-apoptotic actions differ among cell types, at least when studied in culture. Studies of IGF-I anti-apoptotic effects *in vivo* are essential, therefore, to clarify the mechanisms by which IGF-I influences apoptosis.

Apoptosis leads to a massive loss of granule cells during active neurogenesis in the first three postnatal weeks of cerebellar development (Landis and Sidman, 1978; Wood et al., 1993). Because IGF-I overexpression in IGF-II/IGF-I Tg mice occurs when cerebellar apoptosis is active, study of these Tg mice is especially useful to probe IGF-I anti-apoptotic effects. We hypothesized that cerebellar overgrowth in these Tg mice is attributable, at least in large part, to IGF-I inhibition of granule cell apoptosis and that these IGF-I actions are regulated by alterations in the expression of genes for the Bcl family of proteins.

MATERIALS AND METHODS

Reagents. PCR reagents, DNA polymerase, digoxigenin and biotin-labeled nucleotides, digoxigenin chemiluminescent detection reagents, and positively charged nylon membranes were purchased from Roche Molecular Biochemicals (Indianapolis, IN). Reverse transcriptase, RNA polymerase and restriction enzymes were purchased from Promega (Madison, WI), and a purification system for PCR products was purchased from Qiagen (Chatsworth, CA). Reagents for RNase protection assay (RPA) and detection system were obtained from Ambion (Austin, TX). Trizol for RNA extraction was purchased from Life Technologies (Grand Island, NY). Polyvinylidene difluoride (PVDF) membranes, protein molecular standards, and ECL ^{plus} chemiluminescent system for Western immunoblots were from Amersham (Arlington Heights, IL), rabbit polyclonal antibodies against Bcl-x, Bax, Bad, Poly(ADP-ribose) polymerase (PARP), and caspase-3 were from Santa Cruz Biotechnology (Santa Cruz, CA), and Bcl-2 was from Upstate Biotechnology (Lake Placid, NY).

Tg mice. Generation of IGF-II/IGF-I Tg mice has been described in detail elsewhere (Ye et al., 1996). They were bred as heterozygotes and maintained in a vivarium with 12 hr (light/dark) cycles at 22°C. All procedures used were approved by appropriate committees at the University of North Carolina at Chapel Hill.

Brains from IGF-II/IGF-I Tg mice and their normal, non-Tg littermates were collected at P7, P14, and P21 ($n \geq 5$ for most experiments). Tg mice were identified by Northern hybridization analysis of total RNA prepared from the cerebral cortex (the transgene is expressed in all brain regions at all postnatal ages), as previously described (Chrysis and Underwood, 1999). Briefly, 20 μg of total RNA were electrophoresed in 1.2% formaldehyde–agarose gel, transferred to positively charged membranes, and UV cross-linked. Membranes were hybridized with digoxenin-labeled RNA probes transcribed from the human IGF-I cDNA used in transgene, washed at high stringency, and detected by chemiluminescence. Transgene transcripts were observed in multiple sizes of ~2.8, 1.2, and 0.9 kb, as described previously (Ye et al., 1996) and were much more abundant than endogenous IGF-I mRNA.

Detection of apoptosis. Apoptotic cells in CB of Tg mice and their normal littermates were identified by terminal deoxynucleotidyl transferase-mediated deoxy-UTP nick end labeling (TUNEL), according to the manufacturer's instructions (Oncor, Gaithersburg, MD). Briefly, mice were perfused with 4% paraformaldehyde in 0.1 M PBS. The brainstem was transected in the transverse plane just rostral to the pons, and both the brainstem and CB were removed as a single piece. After paraffin embedding, serial sections were cut at a thickness of 5 μm, and every sixth section in the series was mounted on glass slides. Deparaffinized and rehydrated sections were treated with proteinase K (15 μg/ml) at 37°C for 10 min, and endogenous peroxidase activity was blocked with 3% hydrogen peroxide. Slides were then placed in equilibrating buffer and incubated in a reaction buffer containing TdT and dUTP for 60 min at 37°C. After rinsing, slides were incubated with peroxidase-conjugated anti-digoxigenin (introduced together with Triton X-100 and a blocking agent). The sections were then exposed to 0.5 mg/ml diaminobenzidine and 0.05% hydrogen peroxide to generate a brown reaction product and covered with Crystal/Mount (Biomeda, Foster City, CA). At least six sections, 25 μg apart (to avoid counting the same cells twice) were used to determine the number of apoptotic cells. For each section, cerebellar two-dimensional maps were traced using a camera lucida. Completed maps were then digitized and measured using the Image-Pro image analysis system (Media Cybernetics, Silver Spring, MD). The number of apoptotic cells in each cerebellar section was counted. Apoptotic cell number was expressed as a function of cell density (cells per square millimeter).

RPA. Probe template cDNAs for mouse cyclophilin, Bcl-x, Bax, and Bcl-2 were purchased from Ambion. The Bcl-x riboprobe can protect fragments of 60–80 nucleotide (nt) and 215 nt corresponding to Bcl-x short (Bcl-x_S) and long (Bcl-x_L), respectively. The Bax protects a 167 nt fragment, Bcl-2 protects a 191 nt fragment, and the cyclophilin protects a 103 nt fragment. A mouse Bad cDNA of 419 bp was prepared by reverse transcription of mouse brain RNA, followed by amplification by PCR using primers designed according to the published sequence (Yang et al., 1995). The antisense primer was 5′-CTAAGCTCCTCCTCCATCCC-3′ (nucleotides 834–853), and the sense primer was 5′-AGGACTTATCA-GCCGAAGCA-3′ (nucleotides 434–453). The T3 promoter consensus sequence was linked to the 5′-end of the antisense primer, and the T7 promoter consensus sequence was linked to the 5′-end of the sense primer. PCR yielded one fragment at expected size that was then amplified and purified. Purified product was digested with the appropriate restriction enzymes to confirm its identity. Riboprobes were prepared by *in vitro* transcription and purified on 5% acrylamide/8 M urea gel.

RPA was performed as reported previously (Chrysis et al., 1998). Briefly, 20 μg samples of CB total RNA were hybridized overnight at 45°C with biotin-labeled riboprobes (3 fmol of cyclophilin, 2.5 fmol of Bcl-x and Bax, or 3 fmol of cyclophilin, 3 fmol of Bad, and 2 fmol of Bcl-2). After hybridization, samples were treated with A and T1 RNases, and protected fragments were separated in 8% acrylamide/8 M urea gels and transferred to positively charged membranes by electroblotting. After washing, the signal was detected according to manufacturer's recommendations (Ambion). Pilot experiments using constant amount of probes but different concentrations of RNA confirmed that the concentration of probes was in molar excess. Yeast RNA hybridized with the above probes confirmed that the digestion was complete. Bcl-x and Bax were studied in the same reaction because their protected bands can be easily distinguished on the basis of size, and their abundances are similar. Protected bands for Bcl-2 and Bad were much less abundant, requiring longer exposure times to develop their signals, and thus, they were studied together in the same reaction. The signal for each protected band was normalized to that of cyclophilin and expressed as the ratio to the cyclophilin signal.

Western immunoblot. Total protein extracted from the CB with the modified RIPA buffer (Tris–HCl 50 mM, pH 7.4, NP-40 1%, Na-deoxycholate 0.25%, NaCl 150 mM, EDTA 1 mM, PMSF 1 mM, aprotonin, leupeptin, and pepsatin, 1 μg/ml each, Na_3VO_4 1 mM, NaF 1 mM) was measured according to the Bradford method (Bio-Rad, Hercules, CA). Equal amounts of proteins (30 μg for Bcl-x, Bax, Bad, and PARP; 40 μg for caspase-3 at P7 and 60 μg at P14 and P21; and 120 μg for Bcl-2 detection) were fractionated by 12% (or 8% for PARP) SDS-PAGE under reducing conditions. Resolved proteins were electrophoretically transferred to PVDF membranes, blocked overnight at 4°C in NAP-Sure (Geno Technology, St. Louis, MO) diluted 1:1 in Tris-buffered saline (TBS; 10 mM Tris and 150 mM NaCl, pH 7.5). They were then incubated with primary antibodies (antibodies against Bcl-x, Bad, Bax, PARP, and caspase-3 at 1:2000, and antibody against Bcl-2 at 1:3500) in a 1:3 dilution of NAP-Sure/TBS at room temperature for 1 hr, washed in TBS with 0.1% Tween 20 several times, and incubated with horseradish peroxidase-conjugated anti-rabbit Ig (Transduction Laboratories, San Diego, CA) at 1:10,000 dilution. The antigen–antibody complexes were

then detected by chemiluminescence. After development of films, blots were stained with Coomassie blue to assure equal loading of total protein. All experiments were repeated at least twice using two different group of mice.

Statistics. Data were calculated as means and SDs, and results were analyzed by Student's *t* test. p values <0.05 were considered statistically significant.

RESULTS

Apoptosis during postnatal cerebellar development

To assess whether IGF-I overexpression alters apoptosis during cerebellar development, we used the TUNEL method to identify apoptotic cells at P7, P14, and P21. At P7 IGF-I Tg mice had significantly fewer apoptotic cells compared with their normal littermates (Fig. 1; 35.4 ± 11.3 cells/mm^2 in Tg mice and 66.7 ± 6.7 in littermate controls; $p < 0.01$). At P14, Tg mice also exhibited a decrease in apoptotic cell number (16.0 ± 1.9 cells/mm^2 in Tg mice, compared with 37.5 ± 16.6 cells/mm^2 in controls), but the statistical significance was marginal ($p = 0.09$) because of the variability in normal littermates. Apoptotic cells were located mostly in the external granule layer (EGL). There were fewer apoptotic cells in the internal granule layer (IGL). Compared with P7 and P14, the number of apoptotic cells at P21 was markedly decreased in both Tg and controls. Nonetheless, Tg animal tended to have fewer apoptotic cells (0.57 ± 0.2 cells/mm^2 in Tg mice, compared with 1.24 ± 0.5 cells/mm^2 in controls, $p = 0.14$). At this time, most apoptotic cells were located in the internal granule layer.

Caspases

Because caspases are thought to be the ultimate effectors of apoptosis in many situations, we investigated the abundance of caspase-3 to determine whether IGF-I modulates its expression in the CB during early postnatal development. Western immunoblots for caspase-3 revealed that pro-caspase-3 was decreased in CBs from Tg mice at all ages studied, compared with normal littermates (Fig. 2 shows data from Tg mice expressed as a percentage of that in normal, control mice). This finding was consistent in several experiments from different groups of mice. The decrease in pro-caspase-3 in Tg mice does not reflect increased consumption of pro-caspase-3, however, because Tg mice also exhibited comparable decreases in caspase-3, the 20 kDa procaspase-3 cleavage product. More specifically, at P7 pro-caspase-3 was decreased by 59% in Tg mice (302 ± 42 arbitrary units in Tg mice, compared with 512 ± 74 in controls; mean ± SD; $p < 0.05$), whereas the 20 kDa fragment was decreased by 77% (120 ± 30, compared with 533 ± 111 in controls; $p < 0.01$); at P14 pro-caspase-3 was decreased 63.5% in Tg mice (343 ± 65, compared with 940 ± 137 in controls; $p < 0.01$), and the cleavage product was decreased by 68% (225 ± 53, compared with 571 ± 97 in controls; $p < 0.05$); and at P21 these respective decreases were 60% (113 ± 46, compared with 286 ± 35; $p < 0.05$) and 52% (32 ± 6, compared with 67 ± 13; $p < 0.05$) (Fig. 2). During early postnatal cerebellar development, therefore, IGF-I overexpression appears to decrease the expression of pro-caspase-3 without an apparent alteration in its activation, as judged by the relative abundance of its cleavage product.

PARP

PARP, a 116 kDa protein, is a substrate for caspases and cleaved during apoptosis to an 85 kDa fragment. To obtain a measure of caspase activity, therefore, we assessed the abundance of PARP and its caspase-cleaved product. The abundance of 116 kDa PARP decreased during normal cerebellar development (Fig. 3*A*). The relative abundance of the 85 kDa fragment, however, was not concordant with that of 116 kDa PARP, because its abundance was lower at P14 than at P7 and P21. The latter finding suggests that PARP is less actively cleaved at this time. The abundance of 116 kDa and 85-kDA PARP in Tg mouse CBs changes in a similar manner (Fig. 3*B*).

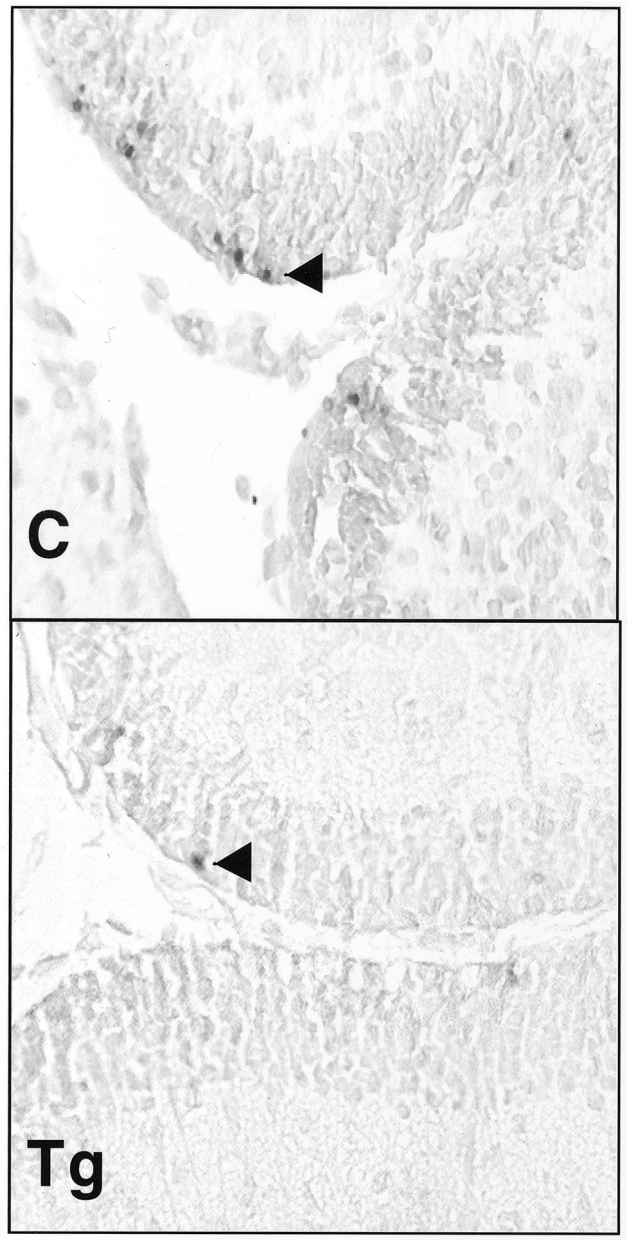

Figure 1. Representative microphotographs from TUNEL assay in CBs from control (*C*) and IGF-I overexpressing transgenic (*Tg*) mouse at P7. CBs from P7 Tg animals had a 47% decrease in the number of apoptotic cells.

Compared with normal controls, P7 Tg mice exhibited a 76% decrease in 85 kDa PARP fragment ($p < 0.05$) without a significant change in the abundance of the uncleaved protein (Fig. 4*A* shows representative Western blots, and *B* depicts the abundances of 85 and 116 kDa PARP in Tg mice expressed as a percentage of that in control mice). The ratio of 85 kDa to 116 kDa PARP in P7 Tg mice, therefore, was 25% (0.112 ± 0.015) of

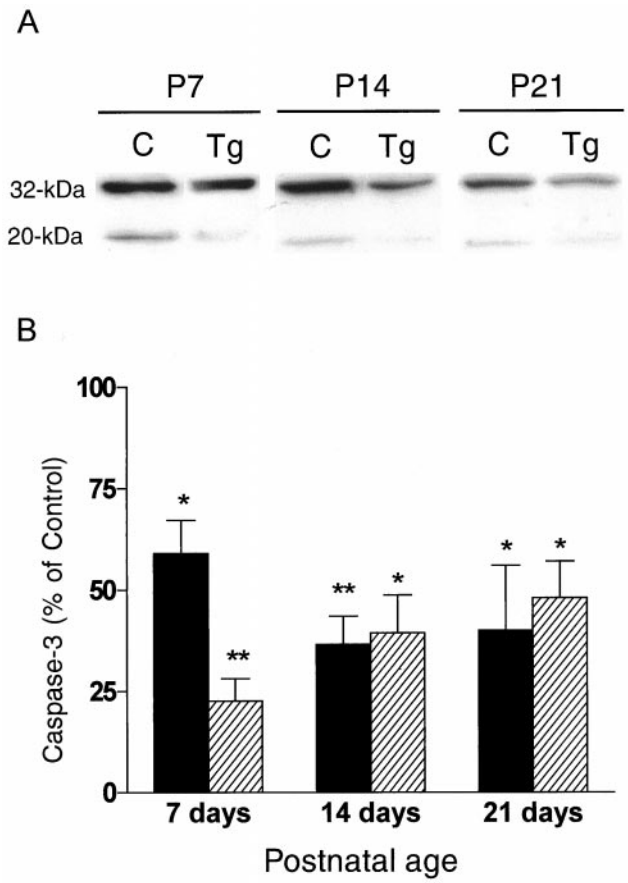

Figure 2. Pro-caspase 3 (32 kDa) and its cleaved fragment caspase-3 (20 kDa) in Tg mice and their normal littermates during cerebellar development. *A* shows representative Western immunoblots from Tg mice and their normal littermates (controls) at P7, P14, and P21. *B,* Chemiluminescent signals were scanned for pro-caspase 3 (*black bars*) and its 20 kDa cleaved fragment (*hatched bars*) from P7, P14, and P21 Tg and control mice. For each developmental age studied, arbitrary optical density units for Tg mice are expressed as a percentage of control. Values represent the mean ± SD; $^{*}p < 0.05$; $^{**}p < 0.01$.

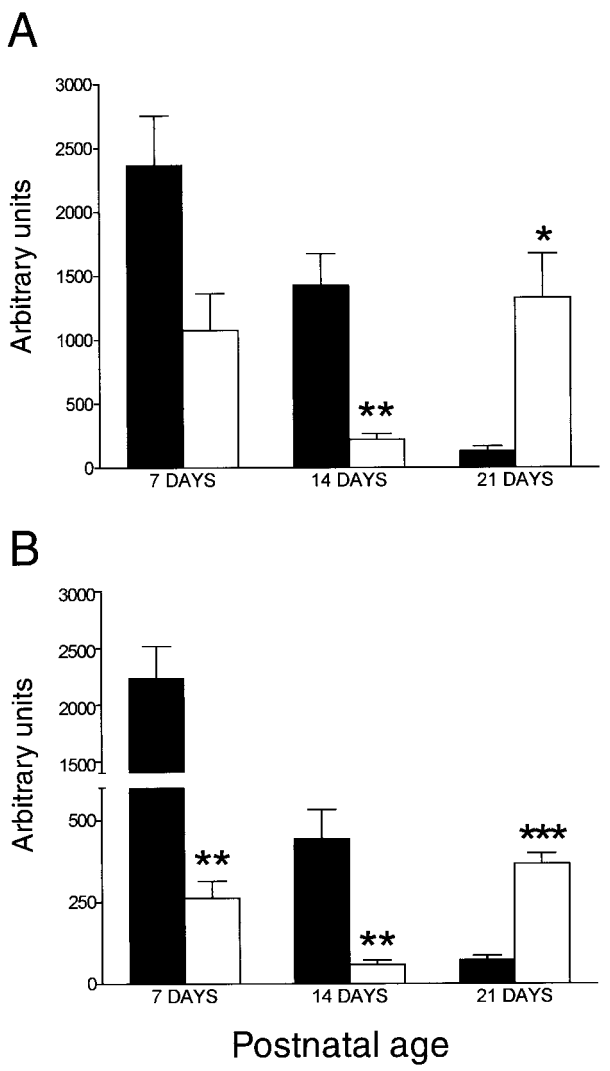

Figure 3. Changes in PARP abundance in Tg and normal mice during CB development, as assessed by Western immunoblot. *A,* Developmental changes of PARP (*black bars*) and its 85 kDa cleaved fragment (*white bars*) in CBs from control mice. Values represent the mean ± SD of arbitrary units derived from chemiluminescent signals. *B,* Developmental changes of PARP (*black bars*) and its 85 kDa cleaved fragment (*white bars*) in CBs from Tg mice. Values represent the mean ± SD of arbitrary units derived from chemiluminescent signals. $^{*}p < 0.05$; $^{**}p < 0.01$; $^{***}p < 0.001$.

the ratio in controls (0.45 ± 0.03; $p < 0.0001$). This lower ratio in Tg mice is likely to reflect decreased 116 kDa cleavage, and in turn decreased caspase activity. At P14 both the 85 kDa cleaved fragment and intact PARP were significantly reduced in Tg mice (by 73 and 69%, respectively; $p < 0.01$), but the 85 to 116 kDa PARP ratio was not significantly reduced (87% of control; 0.13 ± 0.016 in Tg mice and 0.15 ± 0.02 in controls). At P21, both 85 kDa and 116 kDa PARP remained decreased (73 and 45% decreases, respectively), but the differences in the 116 kDa PARP did not meet tests of statistical significance. The ratio of 85 to 116 kDa PARP, however, was reduced by 50% in Tg mice (5 ± 0.6), compared with controls (10 ± 1.6; $p < 0.0001$). These findings suggest that IGF-I overexpression reduces PARP expression in the CB during development. In addition, it seems likely that the decrease in the abundance of p85 kDa PARP relative to that of 116 kDa PARP at P7 and P21 reflects reduced caspase activity.

IGF-I overexpression modulates the Bcl family of gene expression

The Bcl family of proteins, named for the prototype Bcl-2 gene, are intimately involved in the regulation of apoptosis. Bcl proteins, such as Bcl-2 and Bcl-x_L, exert anti-apoptotic effects, whereas others have proapoptotic actions, e.g., Bax, Bad and Bcl-x_S. To determine whether IGF-I altered their expression in a manner consistent with IGF-I anti-apoptotic actions, we determined the mRNA and protein abundance of Bcl family members with different apparent actions on apoptosis. At each age studied during cerebellar development, the expression of Bcl-2 and Bad (both mRNA and protein) was markedly less than that of Bcl-x and Bax. These differences in abundance necessitated using different experimental conditions (e.g., differing exposure times for RPAs and differing amounts of proteins for western immunoblots) for each measure, and thus, only direct comparisons between Tg and normal CBs could be made, i.e., quantitative comparisons among Bcl proteins during development were not possible.

We obtained data on the expression of two anti-apoptotic Bcl family members, Bcl-2 and Bcl-x_L. Although the Bcl-x riboprobe used could detect both Bcl-x_L (a 215 nt band) and Bcl-x_S (60–80

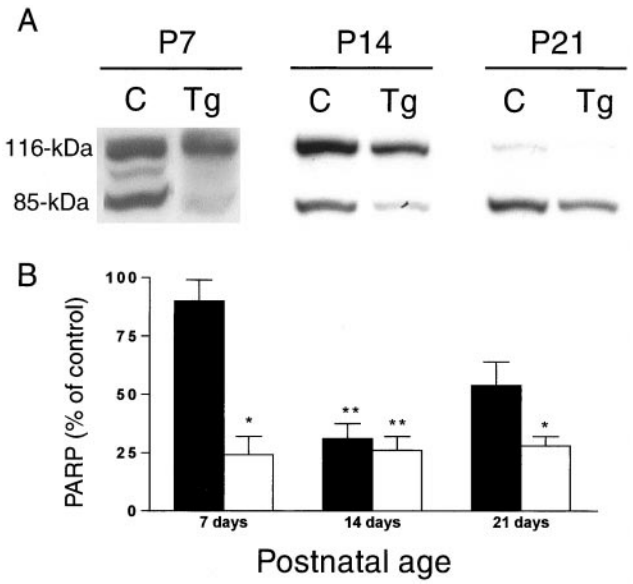

Figure 4. PARP protein from CBs of Tg and normal littermates, assessed by Western immunoblot. *A* shows representative Western immunoblots of 116 kDa PARP and its 85 kDa cleavage fragment in CBs from normal controls (*C*), and Tg mice at P7, P14, and P21. *B,* The abundance (mean ± SD) of PARP and its 85 kDa fragment in Tg CBs expressed as a percentage of that in their normal littermates. $^{*}p < 0.05$; $^{**}p < 0.01$.

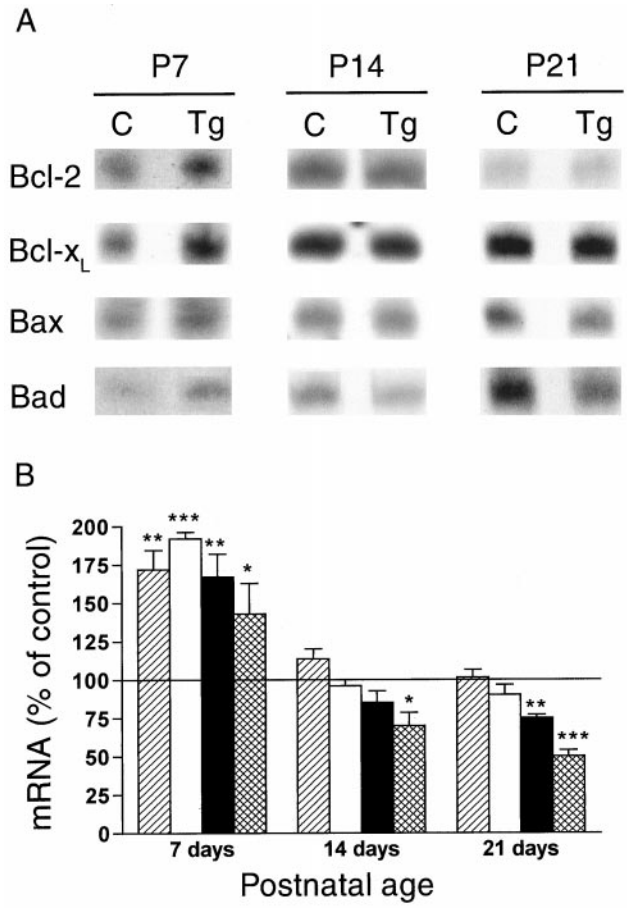

Figure 5. Effects of IGF-I overexpression on Bcl-x_L Bcl-2, Bax, and Bad mRNAs assessed by RPA. *A,* Biotin-labeled gel-purified Bcl-x, Bax, and mouse cyclophilin riboprobes were cohybridized with 20 μg of total RNA from CBs. Each of the protested bands was of the expected size, i.e., 201, 167, and 100 nt, respectively. Bad, Bcl-2, and cyclophilin riboprobes also were cohybridized with 20 μg of total RNA giving bands of the expected sizes (491, 191, and 100 nt, respectively). *B*, Autoradiographic signals were scanned, normalized to those from cyclophilin, and expressed as a ratio of the signal to that of cyclophilin. Data (mean ± SD) from Tg mice is expressed as a percentage of their normal littermates. *Hatched bars* represent Bcl-2, *white bars* Bcl-x, *black bars* Bax, and *cross-hatched bars* Bad. $^{*}p < 0.05$; $^{**}p < 0.01$; $^{***}p < 0.001$.

nt), no signals for the Bcl-x_S transcript were detected in either Tg or normal mice at any age studied. Consistent with this finding, only the 29 kDa Bcl-x_L protein was detected by Western analysis. Compared with their normal littermates at P7 (Fig. 5), Bcl-x_L mRNA abundance was increased by 92% in Tg mice (0.27 ± 0.006 arbitrary units, compared with 0.14 ± 0.01 in controls; mean ± SD; $p < 0.001$) and that of Bcl-x_L protein by 134% (2088 ± 314 arbitrary units, compared with 892 ± 183; $p = 0.01$; Fig. 6), whereas at P14 and P21 both mRNA and protein for Bcl-x_L were similar in Tg and their normal littermates (at P14: 0.25 ± 0.01 in Tg mice, compared 0.26 ± 0.01 in controls, p = NS, and 1749 ± 115 in Tg mice, compared with 1792 ± 308 in controls, p = NS, respectively; and at P21: 0.405 ± 0.03 in Tg mice, compared with 0.451 ± 0.017, p = NS; and 1670 ± 78 in Tg mice, compared with 1931 ± 123 in controls, p = NS, respectively).

At P7 Bcl-2 mRNA abundance in Tg mice also was increased (72%; 0.1798 ± 0.013 arbitrary units, compared with 0.1043 ± 0.001; $p < 0.01$), but at P14 and P21 its abundance did not differ from that of control mice (0.168 ± 0.01 in Tg mice, compared with 0.148 ± 0.005 in controls, and 0.209 ± 0.010 in Tg mice, compared with 0.206 ± 0.01, respectively; p = NS; Fig. 5). The abundance of Bcl-2 protein was very low in Tg and control CBs, and thus, quantification was not possible. At P7, however, Bcl-2 abundance appeared to be increased in Tg mice. At P14 and P21 Bcl-2 protein was even less abundant, and no differences could be discerned between Tg and normal CBs.

Changes in the expression of proapoptotic Bcl family members also were observed in Tg mice. At P7 Bax mRNA was increased by 67% (0.066 ± 0.006 arbitrary units in Tg mice, compared with 0.04 ± 0.004 in controls; $p < 0.01$; Fig. 5), but Bax protein was unchanged (524 ± 68 in Tg mice, compared with 568 ± 103 in controls; p = NS; Fig. 6). At P14 Bax mRNA was unchanged (0.112 ± 0.01 in Tg mice, compared with 0.132 ± 0.005; p = NS), but protein abundance was decreased by 35% in Tg mice (776 ± 125 in Tg mice, compared with 1187 ± 126; $p < 0.05$), whereas at P21 both Bax mRNA (0.185 ± 0.004 in Tg mice, compared with 0.245 ± 0.012; $p < 0.01$) and protein abundance (913 ± 152 in Tg mice, compared with 3816 ± 646; $p < 0.01$) were decreased in Tg mice (by 25 and 75%, respectively), compared with normal littermates.

Bad mRNA was increased by 43% in P7 Tg mice (0.600 ± 0.08 arbitrary units in Tg mice, compared with 0.391 ± 0.03; $p < 0.05$). Bad protein abundance was similar in Tg and normal mice (996 ± 289 in Tg mice, compared with 902 ± 172; p = NS), but marked variations in protein abundance were observed, especially in Tg mice. In five different experiments from three different groups of mice, Bad protein was found to be either unchanged or moderately increased (by up to 35%) in Tg mice, but because of the high variability in Tg mice, these findings were not significant. Bad

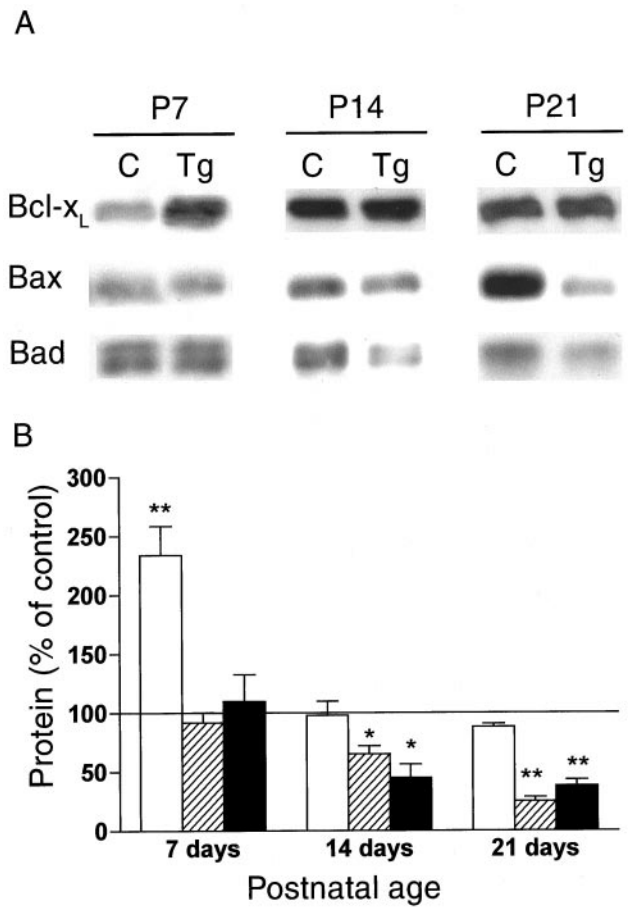

Figure 6. Effects of IGF-I overexpression on the Bcl-x_L, Bax, and Bad proteins assessed by Western immunoblot in CBs from P7, P14, and P21 Tg mice and their normal littermates. *A* shows representative Western immunoblots of Bcl-x, Bax, and Bad in CBs from Tg and normal (*C*) mice at P7, P14, and P21. *B,* Data (mean ± SD) from Tg mice is expressed as a percentage of their normal littermates. *White bars* represent Bcl-x, *hatched bars* Bax, and *black bars* Bad.

immunostaining at P7 revealed doublet bands. It is likely that one of these bands represents phosphorylated Bad. The resolution of the doublets on our gels did not permit quantification of each separately. We, however, had the impression that the abundance of the lower band was more variable and may have accounted for the variability of Bad abundance, especially in Tg CBs. At P14 Bad mRNA abundance was decreased by 36% in Tg mice (0.48 ± 0.06 in Tg mice, compared with 0.68 ± 0.03; $p < 0.05$), and protein abundance was decreased by 47% (441 ± 80 in Tg mice, compared with 803 ± 176; $p = 0.036$). At P21 Bad mRNA was decreased by 50% (0.093 ± 0.0020 in Tg mice, compared with 0.186 ± 0.017; $p < 0.001$) and protein by 62% (231 ± 45 in Tg mice, compared with 604 ± 74; $p < 0.01$). Doublet Bad immunostaining was not obvious at P14 and not observed at P21.

Our results demonstrate that IGF-I overexpression in the postnatal CB alters Bcl family gene expression in a developmentally specific manner. At P7 the abundance of each Bcl mRNA was significantly increased, but only Bcl-x_L protein abundance was increased, whereas at P14 and P21, Bax and Bad expression were decreased. Each of these changes is consistent with IGF-I anti-apoptotic actions, and changes in protein abundance are concordant with the inhibition of apoptosis.

DISCUSSION

We report that postnatal cerebellar IGF-I overexpression attenuates the apoptosis occurring in granule cells during cerebellar development. Greater than 85% of the apoptotic cells identified were in granule cell layers, and IGF-I inhibition of apoptosis was similar in both the EGL and IGL. We believe that IGF-I derived from Purkinje cells exerts anti-apoptotic actions directly on granule cells, because the transgene (Ye et al., 1996), like the native gene (Bondy and Lee, 1993), is expressed by Purkinje cells and because IGF-I has been shown to inhibit apoptosis in primary cultures of granule cells (D'Mello et al., 1993; Leski et al., 2000). Our data, however, do not exclude indirect IGF-I effects on granule cells. IGF-I-induced decreases in apoptosis are associated with alterations in the expression of the Bcl family of proteins. Furthermore, altered Bcl expression occurs in a developmentally specific manner, such that in early postnatal life (P7) there is increased expression of the anti-apoptotic genes, Bcl-x_L and Bcl-2, whereas at later ages (P14 and P21) the expression of proapoptotic proteins, Bax and Bad, is decreased. These changes are associated with decreases in the expression of procaspase-3 and the active enzyme, caspase-3, and decreased caspase-3 activity, as judged by decreased abundance of the 85 kDa PARP cleavage product.

Between P5 and P9 of rodent cerebellar development, granule cells undergo a major wave of classical apoptosis, i.e., programmed cell death characterized by DNA fragmentation, (Landis and Sidman, 1978; Wood et al., 1993). As judged by TUNEL, we found that postnatal cerebellar IGF-I overexpression attenuates apoptosis significantly during this time (P7). Inhibition of premitotic granule cells apoptosis at P7 could result in a large increase in granule cell number, especially if all or most such cells subsequently undergo one or more rounds of division. Given that granule cell apoptosis was decreased in throughout both the EGL and IGL of Tg mice, IGF-I likely inhibits apoptosis of both premitotic and in postmitotic cells. Our study, however, was not designed to address this question.

Although not meeting tests of statistical significance, CBs from Tg mice had ~50% fewer apoptotic cells at P14 and P21. A number of other lines of evidence, however, strongly suggest that IGF-I overexpression inhibits apoptosis at ages beyond the first week of postnatal development: (1) cerebellar overgrowth in IGF-I Tg mice continues until adulthood, despite the fact that our previous studies only detected evidence of small increases in granule cell proliferation (~10%) at one time during postnatal development (P15) (Ye et al., 1996); (2) the abundance of the 85 kDa fragment of PARP, which can result from caspase cleavage during apoptosis, is significantly reduced in CBs from Tg mice at P21; (3) both procaspase 3 and its active fragment are significantly decreased at P21, suggesting decreased apoptotic activity; and (4) the abundance of the proapoptotic proteins Bax and Bad are significantly decreased in CBs from Tg mice at P14 and P21. More detailed morphometric studies will be necessary to determine the times when IGF-I anti-apoptotic actions have their greatest impact on granule cell number.

PARP synthesizes poly-ADP-ribose from nicotine amid dinucleotide in response to DNA strand breaks and is involved in many genomic processes, including DNA base excision repair (Satoh et al., 1994) and DNA replication (Yoshida and Simbulan, 1994). PARP was one of the first substrates shown to be cleaved by caspases. Although its role in apoptosis is not clear, a reduction in PARP cleavage can be taken as evidence of decreased

apoptosis resulting from decreased caspase activity. Our findings of decreases in the abundance of procaspase-3 and its activated enzyme at each age studied are consistent with the latter speculation. A reduction in caspase activity, thus, could account for the decrease in cleaved PARP and represent a downstream mechanism for IGF-I anti-apoptotic actions. Relative to littermate controls, we found a decrease in cleaved PARP in the CBs of Tg mice at each time studied, as well as decreased PARP expression at P14. We also observed that PARP abundance decreased in normal mice during this period of cerebellar development. The progressive decrease in PARP expression, therefore, also might be a reflection of the normal diminution in cell proliferation, and consequently decreased requirement for DNA repair, which occurs during the same period.

At P7 before the expression of the IGF-I transgene has reached its peak [peak abundance occurs by ~P20 (Ye et al., 1996)], mRNA and protein abundances for the anti-apoptotic Bcl-2 and Bcl-x_L are increased. The anti-apoptotic actions of Bcl-2 and Bcl-x_L are well established in cultured neurons (Batistatou et al., 1993; Allsopp et al., 1993, 1995; de Luca et al., 1996) and *in vivo* models (Martinou et al., 1994; Farlie et al., 1995; Gonzalez-Garcia et al., 1995; Motoyama et al., 1995; Michaelidis et al., 1996; Zanjani et al., 1996, 1997). We speculate, therefore, that the increase of Bcl-2 and Bcl-x_L in CBs from Tg mice contributes to the decreased apoptosis found in these mice at P7. The induction of Bcl-2 and Bcl-x_L mRNAs and their proteins by IGF-I overexpression is consistent with *in vitro* studies showing that IGF-I induces Bcl-2 promoter activation (Pugazhenthi et al., 1999) and expression of the Bcl-x_L gene product in PC12 cells (Parrizas and LeRoith, 1997). The upregulation of Bcl-2 and Bcl-x_L expression, however, appeared to be specific to the stage of development, because we observed no difference between Tg and normal mice at P14 or P21. Although we have no explanation for the latter, it seems possible that the failure of IGF-I to increase Bcl-2 and Bcl-x_L expression at later ages could reflect a compensatory mechanism. This speculation is consistent with the finding that IGF-I-induced Bcl-x_L expression in cultured PC12 cells exhibits peaks 3 and 24 hr after IGF-I exposure, but then declines (Parrizas and LeRoith, 1997).

Transcription of the Bcl-x gene generates two alternatively spliced mRNAs: a long form, termed BCL-x_L, which encodes a protein with anti-apoptotic activity, and a shorter form, Bcl-x_S, which encodes a proapoptotic protein (Boise et al., 1993). The riboprobe used for RPAs and the antibody used in Western immunoblots each recognize both forms of Bcl-x. We, however, did not detect Bcl-x_S in any experiment. This result is consistent with a report that mouse tissues, including brain, do not express Bcl-x_S mRNA as judged by both S1 nuclease protection assay and PCR (Gonzalez-Garcia et al., 1994).

The expression of the proapoptotic genes Bax and Bad also were affected by IGF-I, but in a manner different from Bcl-2 and Bcl-x_L. At P7 IGF-I increased the mRNA abundance of both, but their protein abundance was not altered at this time, whereas at P14 and P21 IGF-I decreased the expressions of each in a manner that appeared to be progressive with time. Furthermore, the relative decrease in protein abundance appeared greater than the decrease in mRNA abundance, suggesting the possibility of decreased mRNA translation or increased protein degradation. The increase of Bax and Bad mRNAs at P7 in Tg mice seems paradoxical in the view of the IGF-I anti-apoptotic role. We speculate that this may represent an adaptation to the increase in Bcl-2 and Bcl-x_L expression, rather than a direct effect of IGF-I overexpression. As mentioned above, expression of the IGF-I transgene peaks at ~P20, the time when we observed a nadir in Bax and Bad expression. This pattern leads us to speculate that higher IGF-I levels are necessary for IGF-I to modulate the expression of these proapoptotic proteins. Nonetheless, IGF-I actions on Bax and Bad expression may be crucial to its anti-apoptotic actions. Bax is clearly important in regulating apoptosis in the CNS (Gillardon et al., 1995; Krajewski et al., 1995; Miller et al., 1997; Shindler et al., 1997; Vekrellis et al., 1997; Doughty et al., 2000; Selimi et al., 2000) and especially in cerebellar granule cells (Krajewski et al., 1995; Miller et al., 1997; Doughty et al., 2000; Selimi et al., 2000). For example, apoptosis after cerebral ischemia is associated with increased Bax expression in the CB (Doughty et al., 2000). Furthermore, cerebellar granule cells from Bax-deficient mice are resistant to apoptosis (Miller et al., 1997), and Bax deficiency in Lurcher mice rescues granule cells from apoptosis (Doughty et al., 2000; Selimi et al., 2000).

Bad promotes cell death by binding to and blocking the anti-apoptotic activity of Bcl-x_L (Yang et al., 1995). When Bad is phosphorylated, it dissociates from Bcl-x_L, freeing Bcl-x_L to exert its activity as a suppressor of apoptosis. Phosphorylation of Bad takes place after activation of the PI3-K and its downstream target, the serine–threonine kinase Akt (Datta et al., 1997; del Peso et al., 1997). IGF-I-induced neuronal survival has been linked to the activation of the PI3-K pathway and the subsequent inactivation of Bad resulting from Akt phosphorylation (Datta et al., 1997). The antibody we used to detect Bad recognizes both phosphorylated and nonphosphorylated forms, and it is likely that one of the doublet bands noted on P7 Western blots represents phosphorylated Bad. The more slowly migrating band in the doublet was abundant in P7 CBs, but was not detected at P14 or P21. We suspect that this band represents phosphorylated Bad and that the high variability noted in Bad protein levels at P7 in Tg mice are related to dynamic changes in Bad isoforms induced by phosphorylation at this developmental time. A high proportion of phosphorylated Bad would also contribute to the significant reduction in apoptosis that occurs in P7 Tg mice. An antibody specific for phosphorylated Bad would provide more definitive information.

Whereas IGF-I anti-apoptotic effects have been well documented in cultured cells, *in vivo* studies are few. A number of studies indicate that intraventricular IGF-I administration can protect against neuron injury after hypoxia–ischemia (Guan et al., 1996, 2000; Johnston et al., 1996), and Wang et al. (2000) demonstrated that topical IGF-I application on the cerebral cortex can ameliorate apoptosis after ischemia. Recent evidence indicates that systemically administered IGF-I can cross the blood–brain barrier (Armstrong et al., 2000). Furthermore, systemically administered IGF-I appears capable of protecting neuron from injury-induced apoptosis (Tagami et al., 1997). Therefore, IGF-I appears capable of protecting against injury-induced neuron death.

In summary, our data demonstrate that IGF-I attenuates apoptosis during cerebellar development by affecting multiple steps in the apoptotic pathway in a developmentally specific manner. We believe that our data indicates an important role for IGF-I in the normal control of apoptosis during CB development and that it could be useful in the therapy of a variety of neural injuries and disorders.

REFERENCES

Allsopp TE, Wyatt S, Paterson HF, Davies AM (1993) The proto-oncogene bcl-2 can selectively rescue neurotrophic factor-dependent neurons from apoptosis. Cell 73:295–307.

Allsopp TE, Kiselev S, Wyatt S, Davies AM (1995) Role of Bcl-2 in the brain-derived neurotrophic factor survival response. Eur J Neurosci 7:1266–1272.

Armstrong CS, Wuarin L, Ishii DN (2000) Uptake of circulating insulin-like growth factor-I into the cerebrospinal fluid of normal and diabetic rats and normalization of IGF-II mRNA content in diabetic rat brain. J Neurosci Res 59:649–660.

Baker J, Liu J, Robertson EJ, Efstratiadis A (1993) Role of insulin-like growth factors in embryonic and postnatal growth. Cell 75:73–82.

Baker NL, Russo VC, Bernard O, D'Ercole AJ, Werther GA (1999) Interactions between bcl-2 and the IGF system control apoptosis in the developing mouse brain. Brain Res Dev Brain Res 118:109–118.

Baserga R, Resnicoff M, D'Ambrosio C, Valentinis B (1997) The role of the IGF-I receptor in apoptosis. Vitam Horm 53:65–98.

Batistatou A, Merry DE, Korsmeyer SJ, Greene LA (1993) Bcl-2 affects survival but not neuronal differentiation of PC12 cells. J Neurosci 13:4422–4428.

Boise LH, Gonzalez-Garcia M, Postema CE, Ding L, Lindsten T, Turka LA, Mao X, Nunez G, Thompson CB (1993) Bcl-x, a bcl-2-related gene that functions as a dominant regulator of apoptotic cell death. Cell 74:597–608.

Bondy C, Lee WH (1993) Correlation between insulin-like growth factor (IGF)-binding protein 5 and IGF-1 gene expression during brain development. J Neurosci 13:5092–5104.

Carson MJ, Behringer RR, Brinster RL, McMorris FA (1993) Insulin-like growth factor I increases brain growth and central nervous system myelination in transgenic mice. Neuron 10:729–740.

Chrysis D, Underwood LE (1999) Regulation of components of the ubiquitin system by insulin-like growth factor I and growth hormone in skeletal muscle of rats made catabolic with dexamethasone. Endocrinology 140:5635–5641.

Chrysis D, Moats-Staats BM, Underwood LE (1998) Effect of fasting on insulin receptor-related receptor messenger ribonucleic acid in rat kidney. J Endocrinol 159:R9–R12.

D'Ercole AJ, Ye P, Calikoglu AS, Gutierrez-Ospina G (1996) The role of the insulin-like growth factors in the central nervous system. Mol Neurobiol 13:227–255.

D'Mello SR, Galli C, Ciotti T, Calissano P (1993) Induction of apoptosis in cerebellar granule neurons by low potassium: inhibition of death by insulin-like growth factor I and cAMP. Proc Natl Acad Sci USA 90:10989–10993.

Datta SR, Dudek H, Tao X, Masters S, Fu H, Gotoh Y, Greenberg ME (1997) Akt phosphorylation of BAD couples survival signals to the cell-intrinsic death machinery. Cell 91:231–241.

de Luca A, Weller M, Frei K, Fontana A (1996) Maturation-dependent modulation of apoptosis in cultured cerebellar granule neurons by cytokines and neurotrophins. Eur J Neurosci 8:1994–2005.

del Peso L, Gonzalez-Garcia M, Page C, Herrera R, Nunez G (1997) Interleukin-3-induced phosphorylation of BAD through the protein kinase Akt. Science 278:687–689.

Doughty ML, De Jager PL, Korsmeyer SJ, Heintz N (2000) Neurodegeneration in *Lurcher* mice occurs via multiple cell death pathways. J Neurosci 20:3687–3694.

Dudek H, Datta SR, Franke TF, Birnbaum M, Yao R, Cooper GM, Segal RA, Kaplan DR, Greenberg ME (1997) Regulation of neuronal survival by the serine-threonine protein kinase Akt. Science 275:661–665.

Farlie PG, Dringen R, Rees SM, Kannourakis G, Bernard O (1995) bcl-2 transgene expression can protect neurons against developmental and induced cell death. Proc Natl Acad Sci USA 92:4397–4401.

Gillardon F, Wickert H, Zimmermann M (1995) Up-regulation of bax and down-regulation of bcl-2 is associated with kainate-induced apoptosis in mouse brain. Neurosci Lett 192:85–88.

Gonzalez-Garcia M, Perez-Ballestero R, Ding L, Duan L, Boise LH, Thompson CB, Nunez G (1994) bcl-XL is the major bcl-x mRNA form expressed during murine development and its product localizes to mitochondria. Development 120:3033–3042.

Gonzalez-Garcia M, Garcia I, Ding L, O'Shea S, Boise LH, Thompson CB, Nunez G (1995) bcl-x is expressed in embryonic and postnatal neural tissues and functions to prevent neuronal cell death. Proc Natl Acad Sci USA 92:4304–4308.

Guan J, Williams CE, Skinner SJ, Mallard EC, Gluckman PD (1996) The effects of insulin-like growth factor (IGF)-1, IGF-2, and des-IGF-1 on neuronal loss after hypoxic-ischemic brain injury in adult rats: evidence for a role for IGF binding proteins. Endocrinology 137:893–898.

Guan J, Bennet TL, George S, Waldvogel H, Faull RL, Gluckman PD, Keunen H, Gunn AJ (2000) Selective neuroprotective effects with insulin-like growth factor-1 in phenotypic striatal neurons following ischemic brain injury in fetal sheep. Neuroscience 95:831–839.

Johnston BM, Mallard EC, Williams CE, Gluckman PD (1996) Insulin-like growth factor-1 is a potent neuronal rescue agent after hypoxic-ischemic injury in fetal lambs. J Clin Invest 97:300–308.

Jung YK, Miura M, Yuan J (1996) Suppression of interleukin-1 beta-converting enzyme-mediated cell death by insulin-like growth factor. J Biol Chem 271:5112–5117.

Krajewski S, Mai JK, Krajewska M, Sikorska M, Mossakowski MJ, Reed JC (1995) Upregulation of bax protein levels in neurons following cerebral ischemia. J Neurosci 15:6364–6376.

Kulik G, Klippel A, Weber M (1997) Antiapoptotic signalling by the insulin-like growth factor I receptor, phosphatidylinositol 3-kinase, and Akt. Mol Cell Biol 17:1595–1606.

Landis DMD, Sidman RL (1978) Electron microscopic analysis of postnatal histogenesis in the cerebellar cortex of staggerer mutant mice. J Comp Neurol 179:831–863.

Leski ML, Valentine SL, Baer JD, Coyle JT (2000) Insulin-like growth factor I prevents the development of sensitivity to kainate neurotoxicity in cerebellar granule cells. J Neurochem 75:1548–1556.

Liu J, Baker J, Perkins AS, Robertson EJ, Efstratiadis A (1993) Mice carrying null mutations of the genes encoding insulin-like growth factor I (Igf-1) and type 1 IGF receptor (Igf1r). Cell 75:59–72.

Martinou JC, Dubois-Dauphin M, Staple JK, Rodriguez I, Frankowski H, Missoten M, Albertini P, Talabot D, Catsicas S, Pietra C, Huarte J (1994) Overexpression of BCL-2 in transgenic mice protects neurons from naturally occurring cell death and experimental ischemia. Neuron 13:1017–1030.

Matthews CC, Feldman EL (1996) Insulin-like growth factor I rescues SH-SY5Y human neuroblastoma cells from hyperosmotic induced programmed cell death. J Cell Physiol 166:323–331.

Michaelidis TM, Sendtner M, Cooper JD, Airaksinen MS, Holtmann B, Meyer M, Thoenen H (1996) Inactivation of bcl-2 results in progressive degeneration of motoneurons, sympathetic and sensory neurons during early postnatal development. Neuron 17:75–89.

Miller TM, Moulder KL, Knudson CM, Creedon DJ, Deshmukh M, Korsmeyer SJ, Johnson Jr EM (1997) Bax deletion further orders the cell death pathway in cerebellar granule cells and suggests a caspase-independent pathway to cell death. J Cell Biol 139:205–217.

Minshall C, Arkins S, Straza J, Conners J, Dantzer R, Freund GG, Kelley KW (1997) IL-4 and insulin-like growth factor-I inhibit the decline in Bcl-2 and promote the survival of IL-3-deprived myeloid progenitors. J Biol Chem 159:1225–1232.

Motoyama N, Wang F, Roth KA, Sawa H, Nakayama I, Negishi I, Senju S, Zhang Q, Fujii S, Loh DY (1995) Massive cell death of immature hematopoietic cells and neurons in Bcl-x-deficient mice. Science 267:1506–1510.

Parrizas M, LeRoith D (1997) Insulin-like growth factor-1 inhibition of apoptosis is associated with increased expression of the bcl-xL gene product. Endocrinology 138:1355–1358.

Parrizas M, Saltiel AR, LeRoith D (1997) Insulin-like growth factor 1 inhibits apoptosis using the phosphatidylinositol 3′-kinase and mitogen-activated protein kinase pathways. J Biol Chem 272:154–161.

Pugazhenthi S, Miller E, Sable J, Young P, Heidenreich KA, Boxer LM, Reusch JE (1999) Insulin-like growth factor-I induces bcl-2 promoter through the transcription factor cAMP-response element-binding protein. J Biol Chem 274:27529–27535.

Satoh MS, Poirier GG, Lindahl T (1994) Dual function for poly(ADP-ribose) synthesis in response to DNA strand. Biochemistry 33:7099–7106.

Selimi F, Vogel MW, Mariani J (2000) Bax inactivation in Lurcher mutants rescues cerebellar granule cells but not Purkinje cells or inferior olivary neurons. J Neurosci 20:3687–3694.

Shindler KS, Latham CB, Roth KA (1997) Bax deficiency prevents the increased cell death of immature neurons in bcl-x-deficient mice. J Neurosci 17:3112–3119.

Singleton JR, Dixit VM, Feldman EL (1996) Type I insulin-like growth factor receptor activation regulates apoptotic proteins. J Biol Chem 271:31791–31794.

Tagami M, Ikeda K, Nara Y, Fujino H, Kubota A, Numano F, Yamori Y (1997) Insulin-like growth factor-1 attenuates apoptosis in hippocampal neurons caused by cerebral ischemia and reperfusion in stroke-prone spontaneously hypertensive rats. Lab Invest 76:613–617.

Vekrellis K, McCarthy MJ, Watson A, Whitfield J, Rubin LL, Ham J (1997) Bax promotes neuronal cell death and is downregulated during the development of the nervous system. Development 124:1239–1249.

Wang JM, Hayashi T, Zhang WR, Sakai K, Shiro Y, Abe K (2000) Reduction of ischemic brain injury by topical application of insulin-like growth factor-I after transient middle cerebral artery occlusion in rats. Brain Res 859:381–385.

Wood KA, Dipasquale B, Youle R (1993) In situ labeling of granule cells for apoptosis-associated DNA fragmentation reveals different mechanisms of cell loss in developing cerebellum. Neuron 11: 621–632.

Yang E, Zha J, Jockel J, Boise LH, Thompson CB, Korsmeyer SJ (1995)

Bad, a heterodimeric partner for Bcl-XL and Bcl-2, displaces Bax and promotes cell death. Cell 80:285–291.

Ye P, D'Ercole AJ (1999) Insulin-like growth factor I protects oligodendrocytes from tumor necrosis factor-alpha-induced injury. Endocrinology 140:3063–3072.

Ye P, Carson J, D'Ercole AJ (1995) In vivo actions of insulin-like growth factor-I (IGF-I) on brain myelination: studies of IGF-I and IGF binding protein-1(IGFBP-1) transgenic mice. J Neurosci 15:7344–7356.

Ye P, Xing Y, Dai Z, D'Ercole AJ (1996) In vivo actions of insulin-like growth factor-I (IGF-I) on cerebellum development in transgenic mice: evidence that IGF-I increases proliferation of granule cell progenitors. Brain Res Dev Brain Res 95:44–54.

Yoshida S, Simbulan CM (1994) Interaction of poly(ADP-ribose) polymerase with DNA polymerase alpha. Mol Cell Biochem 138:39–44.

Zanjani HS, Vogel MW, Delhaye-Bouchaud N, Martinou JC, Mariani J (1996) Increased cerebellar Purkinje cell numbers in mice overexpressing a human bcl-2 transgene. J Comp Neurol 374:332–341.

Zanjani HS, Vogel MW, Delhaye-Bouchaud N, Martinou JC, Mariani J (1997) Increased inferior olivary neuron and cerebellar granule cell numbers in transgenic mice overexpressing the human Bcl-2 gene. J Neurobiol 31:502–516.

Zhang W, Ghetti B, Lee WH (1997) Decreased IGF-I gene expression during the apoptosis of Purkinje cells in pcd mice. Brain Res Dev Brain Res 98:164–176.